PARAMETRIC TRANSFER-FUNCTIONS FOR PACKED, BINARY DISTILLATION COLUMNS

by

J.B. Edwards* and M. Guilandoust†

A revised paper submitted to the Institution of Chemical Engineers for consideration for publication in the Transactions

February 1982

Research Report No. 170

* Senior Lecturer, Department of Control Engineering, University of Sheffield, Mappin Street, Sheffield S1 3JD.

† Research Student in the same Department.

SYNOPSIS

Using similar assumptions to those adopted in a companion paper[1] for tray column analysis, a parametric transfer-function (T.F.M.) is here derived completely analytically for packed, binary distillation columns. For simplicity, the method of calculation is illustrated for a column that is symmetrical statically and dynamically i.e. having a rectifier vapour/stripping section liquid capacitance ratio c = 1.0. This produces a completely diagonal T.F.M. between the sum and difference of output composition changes and the circulating and product take-off flow rates. The T.F.M. is also presented for $c \neq 1.0$ and, although no longer diagonal at all frequencies, analysis and simulation show that the column behaviour is not greatly affected by changes in this parameter.

Long packed columns are shown to produce novel nonminimum phase effects when twin product control is attempted, whereas serious travelling-wave phenomena can limit controller performance in short columns. The possibility of zero separation-gain is also revealed. The computed shapes of inverse Nyquist loci are confirmed by analysis and by numerical time-domain simulation. The chief cause of discrepancy between tray and packed column behaviour is shown to result from the continuous equilibrium assumption for theoretical trays.

1. Symbols

In the present paper, identical symbols to those used in the preceeding companion paper[1] here have the same physical significance, with the following exceptions:

h - normalised distance (measured from top and bottom of column) $= h'k/V$

and τ - normalised time $= tk/H_v$

Additional symbols used are:

c - ratio of vapour/liquid capacitance in rectifier and stripper respectively.

H_v, H_v' - vapour capacitance p.u. length in rectifier and stripping sections

J - variable defined by equation (62)

k_r, k_s (=k where equal) - evaporation rate constants p.u. length p.u. departure from equilibrium in rectifier and stripping sections.

P - $(1-c)p/2$

q - $\sqrt{(1+c)p(4+p+cp)/4}$ $\quad (=\sqrt{p^2+2p}\ ,\ c = 1.0)$

$\underline{\tilde{Q}}(s)$ - 2x2 matrix defined by equation (33)

$\underline{\tilde{R}}(s)$ - $s^{-1}\underline{\tilde{Q}}(s)$

$\underline{Q}(h)$ - Inverse Laplace transform of $\underline{\tilde{Q}}(s)$

$\underline{Q}^*(h)$ - " " " " $\underline{\tilde{Q}}(-s)$

$\underline{R}(h)$ - " " " " $\underline{\tilde{R}}(s)$

$\underline{R}^*(h)$ - " " " " $\underline{\tilde{R}}(-s)$

T_1, T_2 - time constants defined by equations (65) and (66).

$\underline{r}$ - vector of tilt and total equilibrium composition changes y_e and x_e'

X_e', x_e' - equilibrium liquid mol-fraction in stripping section and small perturbation therein.

Y_e, y_e - equilibrium vapour mol-fraction in rectifier and small perturbation therein.

z_1 - $(G/V)v$

z_2 - $(G/V)\ell$

2. Introduction

In a companion paper[1] Edwards and Tabrizi derived a parametric transfer-function matrix (T.F.M) model for the composition dynamics of long, binary distillation columns of the tray type. Simplifying assumptions were made at the outset and, thereafter, the derivation proceeded completely analytically and without subsequent approximation. Of the initial assumptions, most were those adopted by several previous researchers and involved the piecewise linearisation of the equilibrium curve, constant molar overflow, zero vapour capacitance, parallel equilibrium and operating lines (leading to equal tray-loading). Variation of tray-holdup through hydrodynamic effects was shown not to affect the small-perturbation behaviour of the composition dynamics about the steady-state. The additional assumption made, initially in the interests of ease of analysis, was that of static symmetry, involving equal lengths of rectifier and stripping section, feed-composition coordinates located at the knee of the linearised equilibrium curve, equal vapour and liquid feed rates and nominally equal take-off rates of top and bottom product. Such operating conditions were shown to produce top and bottom products of nominally equal purity, in terms of lighter and heavier component respectively: a condition judged by the authors to represent ideal plant design for the composition control of twin products and therefore a practically useful special case. Although precisely derived for this special case, it is anticipated that the model should still stand as a useful approximation for asymmetric situations, hopefully up to the point where a single- rather than a twin-stage analysis might become more appropriate. Supporting experimental data was given.

In the present paper we apply somewhat similar techniques to packed columns which yield rather more complex equations and important behavioural differences. Additional symmetry assumptions need to be introduced, particularly in respect of liquid and vapour capacitance in the column, to keep algebraic complexity manageable within the confines of a single paper, but final results

are also given for general capacitance ratios. References (2) and (3) must be consulted for their detailed derivation. In the following derivations, assumptions of the type made in the companion paper are not re-justified here. New assumptions are highlighted however where appropriate. After deriving the model we examine some of the plant behaviour predictions it yields.

3. Equilibrium and Material Balance Formulations

The column is illustrated diagramatically in Fig. 1 the rectifier and stripping section being compartmentalised, vertically into counterflow vapour and liquid streams separated by a conceptual inter-phase barrier and horizontally into a number of conceptual cells to which dynamic mass balances may be applied. As before the equilibrium curve is linearised thus:

$$(1-X) = \alpha(1-Y_e) \quad , \qquad \text{rectifier} \tag{1}$$

and

$$Y' = \alpha X'_e \quad , \qquad \text{stripping section} \tag{2}$$

Y_e being the equilibrium value of vapour composition* associated with rectifier liquid of composition X, whilst X'_e is the equilibrium value of liquid composition associated with stripping section vapour of composition Y'. The initial slope of the linearised curve is the constant α.

Taking a material balance for the flow of lighter component through and within an arbitrary cell of the rectifier and stripping section, applying a Taylor expansion and letting cell length $\delta h \to 0$, yields the following partial differential equations (p.d.e's), having eliminated X and Y' using (1) and (2):

$$\partial(H_v Y)/\partial t - V_r \partial Y/\partial h' = k_r(Y_e - Y) \tag{3}$$

$$-\alpha\partial(H_\ell Y_e)/\partial t - L_r \alpha \partial Y_e/\partial h' = k_r(Y_e - Y) \tag{4}$$

$$-\partial(H'_\ell X')/\partial t + L_s \partial X'/\partial h' = k_s(X' - X'_e) \tag{5}$$

$$\alpha\partial(H'_v X'_e)/\partial t + \alpha V_s \partial X'_e/\partial t = k_s(X' - X'_e) \tag{6}$$

where Y and X' are the actual vapour and liquid compositions in rectifier and stripping section respectively, $V_r(V_s)$, $L_r(L_s)$ are the vapour and liquid molar

* The term composition is used throught to mean mol-fraction of the lighter component in the binary mixture.

flow-rates in the rectifier (stripper), $H_v(H'_v)$ $H_\ell(H'_\ell)$ the vapour and liquid capacitances p.u. length and $k_r(k_s)$ the evaporation rate constants p.u. length for the rectifier (stripper). As before, h' denotes the distance to the point in question measured from the end-vessel (accumulator or reboiler).

4. Normalisation

As previously, we shall choose a plant built and operated symmetrically thus

$$V_r = \alpha L_r = L_s = \alpha V_s = V \tag{7}$$

with a mixed feed of vapour, at rate F_v, composition z and liquid at rate F_ℓ, composition Z where

$$F_\ell = F_v = F \tag{8}$$

$$z = \alpha Z = \alpha/(1+\alpha) \tag{9}$$

$$H_v = \alpha H'_v = H_1 \tag{10}$$

$$H'_\ell = \alpha H_\ell = H_2 \tag{11}$$

and, by suitable choice of packing density and section geometry:

$$k_s = k_r = k \tag{12}$$

equation (7) and (8) producing nominally equal product flows (=F) at top and bottom. It should be emphasised however, that equation (7) describes only the nominal (quiescent) operating condition of the plant and does not prevent the application of small, independent changes v,ℓ in, say, V_s and L_r.

Under these conditions the system p.d.e's may be normalised to

$$\begin{aligned} &\partial(cY)/\partial\tau - \partial Y/\partial h = Y_e - Y \\ -\ &\partial Y_e/\partial\tau - \partial Y_e/\partial h = Y_e - Y \\ -\ &\partial X'/\partial\tau + \partial X'/\partial h = X' - X'_e \\ &\partial(cX'_e)/\partial\tau + \partial X'_e/\partial h = X' - X'_e \end{aligned} \tag{13}$$

where normalised time τ and distance h are given by

$$h = h'k/V \tag{14}$$

$$\tau = t\,k/H_2 \tag{15}$$

the base time H_2/k being the time for liquid (in the stripping section) to travel

base distance V/k which may be regarded as the tray spacing of the equivalent tray-column . It has a further physical significance demonstrated in Section 6 . The vapour/liquid capacitance ratio c is defined as

$$c = H_1/H_2 \tag{16}$$

5. Large-Signal Boundary Conditions

5.1 At the feedpoint If L is the normalised length of either section of the columns

$$L = L' k/V \tag{17}$$

then the feed boundary conditions are simply

$$V_s Y'(L) + F_v z = V_r Y(L) \tag{18}$$

and

$$L_r X(L) + F_\ell Z = L_s X'(L) \tag{19}$$

On substituting our chosen symmetrical operating conditions (7) (8) and (9) and eliminating X(L) and Y'(L) in favour of $Y_e(L)$ and $X'_e(L)$ using (1) and (2) we obtain the normalised forms

$$X'_e(L) + \{1 - Y(L)\} = 2/(\alpha+1) \tag{20}$$

and

$$\{1 - Y_e(L)\} + X'(L) = 2/(\alpha+1) \tag{21}$$

5.2 At the end-vessels. Material balances on the accumulator and reboiler (of constant capacitance H_a and H_b moles respectively), yields the differential equations (d.e's)

$$H_a \frac{dX(o)}{dt} = V_r\{Y(o) - X(o)\}$$

or,

$$H_a \frac{\alpha dY_e(o)}{dt} = V_r \left[\alpha\{1 - Y_e(o)\} - \{1 - Y(o)\}\right] \tag{22}$$

and

$$H_b \frac{dX'_e(o)}{dt} = L_s\{X'(o) - Y'(o)\}$$

or

$$H_b \frac{dX'_e(o)}{dt} = L_s\{X'(o) - \alpha X'_e(o)\} \tag{23}$$

assuming the end vessel to run in equilibrium

Again, for symmetry, we set

$$H_a\alpha = H_b = H_e \tag{24}$$

and normalising (22) and (23) then gives

$$T\frac{dY_e(o)}{d\tau} = \alpha\{1 - Y_e(o)\} - \{1 - Y(o)\} \tag{25}$$

and

$$T\frac{dX'_e(o)}{d\tau} = X'(o) - X'_e(o) \tag{26}$$

where

$$T = H_e/V \tag{27}$$

6. Steady-State Solution

The system is now completely specified and steady-state conditions (needed as parameters for the subsequent small perturbation model) may be calculated by setting the time derivatives in (13),(20),(21),(25) and (26) to zero and solving the resulting spatial d.e. subject to its now static boundary conditions. The solutions, given in Fig. 2, for $X'(h)$ $\{= 1 - Y(h)\}$ and $X'_e(h)$ $\{= 1 - Y_e(h)\}$ are linear in h for our chosen symmetrical conditions. We note in particular that the steady-state gradients

$$-\frac{dY}{dh} = -\frac{dY_e}{dh} = \frac{dX'}{dh} = \frac{dX'_e}{dh} = G \tag{28}$$

where, as for the equivalent tray-column, G is again given by

$$G = 2\varepsilon/\{(\alpha+1)(2\varepsilon L + \alpha + 1)\} \tag{29}$$

and that the equilibrium and actual composition profiles are separated by unit normalised distance: i.e. by the base distance V/k in units of h'. This distance therefore now acquires a fuller physical significance. It is interesting also to note that the tray-column solutions[1] for Y and X' are identical to those for Y_e and X'_e in the equivalent packed-column as might be expected since the trays were assumed to operate in continuous equilibrium.

7. Small Perturbation Equations

Implicit differentiation of p.d.e's (3) - (6), writing y, y_e, x', x'_e, v and ℓ for small changes in Y, Y_e, X', X'_e, V_s and L_r respectively and substituting the calculated steady-state values for the remaining upper-case symbols yields the

following normalised small-signal p.d.e's for behaviour around the steady-state, irrespective of hydrodynamic influence on the tower capacitances ($\dot{Y}, \dot{Y}_e, \dot{X}'$ and $\dot{X}'_e$ being zero), viz.

$$\begin{aligned} & c\ \partial y/\partial\tau - \partial y/\partial h + G\ v/V = y_e - y \\ & -\partial y_e/\partial\tau - \partial y_e/\partial h + \alpha G\ell/V = y_e - y \\ & -\partial x'/\partial\tau + \partial x'/\partial h + G\ell/V = x' - x_e' \\ & c\ \partial x_e'/\partial\tau + \partial x_e'/\partial h + \alpha G\ v/V = x' - x_e' \end{aligned} \tag{30}$$

After double Laplace transformation in s w.r.t h and in p w.r.t τ using superscript $\tilde{}$ to denote variable transforms w.r.t. h and τ and $\tilde{}$ to represent transforms w.r.t. τ only, these equations may be written thus

$$\underset{\sim}{Q}^{-1}(s) \begin{pmatrix} \tilde{\tilde{y}} \\ \tilde{y}_e \end{pmatrix} + \begin{pmatrix} \tilde{y}(o) \\ \tilde{y}_e(o) \end{pmatrix} + s^{-1} \begin{pmatrix} 1 & o \\ o & \alpha \end{pmatrix} \begin{pmatrix} \tilde{z}_1 \\ \tilde{z}_2 \end{pmatrix} = \underline{o} \tag{31}$$

and

$$\underset{\sim}{Q}^{-1}(-s) \begin{pmatrix} \tilde{\tilde{x}}'_e \\ \tilde{x}' \end{pmatrix} - \begin{pmatrix} \tilde{x}'_e(o) \\ \tilde{x}'(o) \end{pmatrix} + s^{-1} \begin{pmatrix} \alpha & o \\ o & 1 \end{pmatrix} \begin{pmatrix} \tilde{z}_1 \\ \tilde{z}_2 \end{pmatrix} = \underline{o} \tag{32}$$

$y(o), y_e(o), x'_e(o), x'(o)$ being the transformed variables at h = o and

$$\underset{\sim}{Q}^{-1}(s) = \begin{pmatrix} 1 + cp - s & , & -1 \\ +1 & , & -(1 + p + 2) \end{pmatrix} \tag{33}$$

and $$\left|\tilde{z}_1, \tilde{z}_2\right| = (G/V)\left|\tilde{v}, \tilde{\ell}\right| \tag{34}$$

Now some of the unknowns, say $\tilde{y}_e(o)$ and $\tilde{x}'_e(o)$, may be eliminated at this stage using the small perturbation version of boundary equations (25) and (26) which, after Laplace transformation and normalisation may be expressed:

$$\begin{pmatrix} \tilde{y}_e(o) \\ \tilde{x}'_e(o) \end{pmatrix} = \alpha^{-1} h_e(p) \begin{pmatrix} \tilde{y}(o) \\ \tilde{x}'(o) \end{pmatrix} \tag{35}$$

where $$h_e(p) = 1/(1 + Tp) \tag{36}$$

Performing this elimination and inverting back to the h,p domain, gives, on

substituting L = h, :

$$\begin{pmatrix} \tilde{y}(L) \\ \tilde{y}_e(L) \end{pmatrix} + \tilde{y}(o)\ \underline{Q}(L) \begin{pmatrix} 1 & \\ & \alpha^{-1}h_e \end{pmatrix} + \underline{R}(L) \begin{pmatrix} 1 & o \\ o & \alpha \end{pmatrix} \begin{pmatrix} \tilde{z}_1 \\ \tilde{z}_2 \end{pmatrix} = \underline{o} \qquad (37)$$

and $$\begin{pmatrix} \tilde{x}'_e(L) \\ \tilde{x}'(L) \end{pmatrix} - \tilde{x}'(o)\underline{Q}^*(L) \begin{pmatrix} \alpha^{-1}h_e \\ 1 \end{pmatrix} - \underline{R}^*(L) \begin{pmatrix} \alpha & o \\ o & 1 \end{pmatrix} \begin{pmatrix} \tilde{z}_1 \\ \tilde{z}_2 \end{pmatrix} = \underline{o} \qquad (38)$$

where $\underline{Q}(h)$, $\underline{Q}^*(h)$ are the inverse Laplace transforms (w.r.t. h) of $\tilde{\underline{Q}}(s)$, $\tilde{\underline{Q}}(-s)$ and $\underline{R}(h)$, $\underline{R}^*(h)$ are those of $s^{-1}\tilde{\underline{Q}}(s)$, $-s^{-1}\tilde{\underline{Q}}(-s)$.

The feedpoint boundary conditions (derived by implicit differentiation of (18) and (19) and substitution of the now known steady-state operating conditions) may be expressed thus

$$y(L) = x'_e(L) - (\varepsilon/2)z_1 \qquad (39)$$

and $$x'(L) = y_e(L) + (\varepsilon/2)z_2 \qquad (40)$$

where $$\varepsilon = \alpha - 1 \quad (> o) \qquad (41)$$

so that (39) and (40) may be used to eliminate the feedpoint variables (i.e. at h = L) from (37) and (38) giving

$$\left(\underline{Q}(L) \begin{pmatrix} 1 & \\ & \alpha^{-1}h_e \end{pmatrix}, \underline{Q}^*(L) \begin{pmatrix} \alpha^{-1}h_e & \\ & 1 \end{pmatrix} \right) \begin{pmatrix} \tilde{y}(o) \\ \tilde{x}'(o) \end{pmatrix} = - \left(\underline{R}(L) \begin{pmatrix} 1 & o \\ o & \alpha \end{pmatrix} + \underline{R}^*(L) \begin{pmatrix} \alpha & o \\ o & 1 \end{pmatrix} - \frac{\varepsilon}{2} \begin{pmatrix} 1 & o \\ o & 1 \end{pmatrix} \right) \begin{pmatrix} \tilde{z}_1 \\ \tilde{z}_2 \end{pmatrix} \qquad (42)$$

All variables other than the outputs $\tilde{y}(o)$, $\tilde{x}'(o)$ of main interest, and the inputs $\tilde{z}_1$ and $\tilde{z}_2$ are thus eliminated and matrices $Q(L)$, $Q^*(L)$, $R(L)$ and $R^*(L)$ are readily determined by straightforward Lalpace transform inversion, knowing $\underline{Q}(s)$ from equation (33). It is then a completely straightforward task of matrix algebra to obtain a parametric transfer-function matrix (T.F.M) between $[\tilde{y}(o), \tilde{x}'(o)]^T$ and $[\tilde{v}, \tilde{z}]^T$. Though straightforward, the work required in tedious and must be performed painstakingly to avoid the ever present risk of simple but disastrous errors. Space constraints here demand that we illustrate the method with a simpler special case: that of equal vapour/liquid capacitance i.e.

$$c = 1.0 \tag{43}$$

The additional symmetry that this generates allows considerable simplification of the working involved and yet, as we shall see, does not greatly restrict the scope of the predictions obtained. Results for the general case, $c \neq 1.0$ have been produced by the authors and are given in Section 10. For their detailed derivation, however, interested readers should consult references (2) and (3).

8. T.F.M. Derivation for c = 1

From (33) we deduce that

$$\underset{\sim}{\tilde{Q}}(s) = \frac{1}{\{s + 0.5(1-c)p\}^2 - (cp + c + 1)p - 0.25(1-c)^2p^2} \begin{bmatrix} -(1+p+s) & , & 1 \\ -1, & 1 + cp & s \end{bmatrix}$$

simplifying, for c = 1, to

$$\underset{\sim}{\tilde{Q}}(s) = \frac{1}{s^2 - q^2} \begin{bmatrix} -(1+p+s) & , & 1 \\ -1 & , & 1+p-s \end{bmatrix} \tag{44}$$

where $q^2 = p^2 + 2p$ (45)

thus giving

$$\underset{\sim}{Q}(L), \{\underset{\sim}{Q}^*(L)\} = \begin{bmatrix} -(1+p)(\sinh qL)/q \mp \cosh qL & , & (\sinh qL)/q \\ -(\sinh qL)/q & , & (1+p)(\sinh qL)/q \mp \cosh qL \end{bmatrix} \tag{46}$$

(the top and bottom signs applying to $Q(L)$ and $Q^*(L)$ respectively), from which we obtain the L.H.S of (42) as:

$$\underset{\sim}{Q}(L) \begin{bmatrix} 1 & \\ & \alpha^{-1}h_e \end{bmatrix} \tilde{y}(o) + Q^*(L) \begin{bmatrix} \alpha^{-1}h_e & \\ & 1 \end{bmatrix} \tilde{x}'(o)$$

$$= \begin{bmatrix} a\sinh qL - \cosh qL & , & b\sinh qL - c'\cosh qL \\ -(b\sinh qL - c'\cosh qL) & , & -(a\sinh qL - \cosh qL) \end{bmatrix} \begin{bmatrix} \tilde{y}(o) \\ \tilde{x}'(o) \end{bmatrix} \tag{47}$$

where $a = \{\alpha^{-1}h_e - (1+p)\}/q$, $b = \{1 - \alpha^{-1}h_e(1+p)\}/q$ and $c' = -\alpha^{-1}h_e$

Exploiting the obvious symmetry of (47) we can therefore write

$$\begin{pmatrix} (\alpha^{-1}h_e - 1)(q/p)\sinh qL - (1+\alpha^{-1}h_e)\cosh qL & , & 0 \\ 0 & , & -(1+\alpha^{-1}h_e)(p/q)\sinh qL - (1-\alpha^{-1}h_e)\cosh qL \end{pmatrix} \begin{pmatrix} \tilde{y}(o)-\tilde{x}'(o) \\ \tilde{y}(o)+\tilde{x}'(o) \end{pmatrix}$$

$$= \begin{pmatrix} 1 & 1 \\ 1 & -1 \end{pmatrix} \text{ R.H.S. of equation (42)} \qquad (48)$$

Turning to the R.H.S of (42), $\underline{\tilde{R}}(s)$ is just $s^{-1}\underline{\tilde{Q}}(s)$ and by inverse Laplace Transforms we get

$$\underline{R}(L), \{\underline{R}^{*}(L)\} = q^{-2} \begin{pmatrix} \pm(1+p)(1-\cosh qL) - q\sinh qL & , & \mp(1-\cosh qL) \\ \pm(1-\cosh qL) & , & \mp(1+p)(1-\cosh qL) - q\sinh qL \end{pmatrix} \qquad (49)$$

and after careful manipulation and observation of the system symmetry we obtain

$$\begin{pmatrix} 1 & -1 \\ 1 & -1 \end{pmatrix} \begin{pmatrix} \text{R.H.S.(42)} \end{pmatrix} = \begin{pmatrix} (\varepsilon/p(1-\cosh qL) + (1+\alpha)(\sinh qL)/q + \varepsilon/2 & , & 0 \\ 0 & , & (\varepsilon p/q^2)(1-\cosh qL) + (1+\alpha)(\sinh qL)/q + \varepsilon/2 \end{pmatrix} \begin{pmatrix} \tilde{z}_1+\tilde{z}_2 \\ \tilde{z}_1-\tilde{z}_2 \end{pmatrix} \qquad (50)$$

Combining (48) and (50) therefore yields the T.F.M. relationship

$$\begin{pmatrix} \tilde{y}(o) - \tilde{x}'(o) \\ \tilde{y}(o) + \tilde{x}'(o) \end{pmatrix} = \underline{G}(o,p) \begin{pmatrix} \tilde{v}+\tilde{\ell} \\ \tilde{v}-\tilde{\ell} \end{pmatrix} (G/V) \qquad (51)$$

where $\underline{G}(o,p)$ is diagonal, viz $\underline{G}(o,p) = \begin{pmatrix} g_{11}(o,p) & , & 0 \\ 0 & , & g_{22}(o,p) \end{pmatrix}$ (52)

where $g_{11}(o,p) = \dfrac{(\varepsilon/p)(\cosh qL-1) - (1+\alpha)(\sinh qL)/q - \varepsilon/2}{(1-\alpha^{-1}h_e)(q/p)\sinh qL + (1+\alpha^{-1}h_e)\cosh qL}$ (53)

and $g_{22}(o,p) = \dfrac{(\varepsilon p/q^2)(\cosh qL-1) - (1+\alpha)(\sinh qL)/q - \varepsilon/2}{(p/q)(1+\alpha^{-1}h_e)\sinh qL + (1-\alpha^{-1}h_e)\cosh qL}$ (54)

and, for the static gains, taking limits as $p \to o$ we obtain

$$g_{11}(o,o) = \alpha\{\varepsilon L^2 - (\alpha+1)L - \varepsilon/2\}/\{2\varepsilon L + \alpha + 1\} \qquad (55)$$

and $$g_{22}(o,o) = -\alpha\{(\alpha+1)L + \varepsilon/2\}/\varepsilon \qquad (56)$$

9. Behavioural Predictions

We have thus obtained a completely parametric T.F.M., initially for the special case of c = 1. (The result for any arbitrary value of c is given in Section 10.) From given plant parameters therefore, normalised model parameters L, T, (recall $h_e^{-1}(p) = 1 + Tp$), α and $\varepsilon (= \alpha - 1)$ are readily calculated and, by choosing values of normalised frequency p (set = $j\omega$), frequency-response loci for, say, $g_{11}^{-1}(o,j\omega)$ and $g_{22}^{-1}(o,j\omega)$ may be computed from (53) thro (56). Such loci are given in Section 9.3 and from them the main characteristics of the open-and closed-loop behaviour of the column may be deduced. Much can be learned, however, by inspection and straightforward simplification of equations (53) thro (56) as is now demonstrated.

9.1 Static gains

It is interesting firstly to compare the expressions for $g_{11}(o,o)$, $g_{22}(o,o)$ deduced for packed columns (equations 55 and 56) with these derived in the companion paper for tray-columns, viz:

$$g_{11}(o,o) = \varepsilon(L^2 + L + 0.5)/(2\varepsilon L + \alpha + 1) \qquad (57)$$

and

$$g_{22}(o,o) = -\{(\alpha+1)L + 0.5(3\alpha+1)\}/\varepsilon \qquad (58)$$

The results are clearly very similar for long columns ($L >> 1.0$) but it is important to note the distinction that $g_{11}(o,o)$ can be negative for shorter packed columns. Such columns can still yield practical separations 2GL (see equation (29)). It is however at the high frequency end of the spectrum that major differences between the two columns appear.

9.2 High-frequency (H.F.) behaviour

Noting that , if $p = j\omega$,

$$q \to j\omega + 1 \quad , \qquad 1.0 << \omega \qquad (59)$$

then it is readily shown, from (53) and (54), that

$$\text{Lim}_{1 << \omega << 4/\varepsilon} \{j\omega\, g_{11}(o,j\omega)\} \to -J \quad , \quad T >> 1.0 \qquad (60)$$

$$\text{or} \to -J/\{1 + \exp(-2qL)\,\alpha^{-1}\} \quad , \; T = 0 \qquad (61)$$

where

$$J = 1 - \alpha \exp(-2qL) + \varepsilon \exp(-qL) \qquad (62)$$

The transfer-function g_{11} thus approaches a basically integrating process at high-frequency (H.F), but here the H.F. gain is negative, unlike the tray column where H.F. gain (for g_{11}) is positive.

For long columns separating difficult mixtures (i.e. $\varepsilon << 1.0$ requiring $L >> 1.0$ for a reasonable separation 2GL: see equation 29) the exponential terms in (61) and (62) are clearly negligible but for larger values of ε, necessitating a shorter column for the same separation, the term $\varepsilon\exp(-qL)$ acquires importance. It represents a composition wave reflected from the feed boundary and yields the approximate H.F. transfer function

$$\lim_{1<<\omega<<4/\varepsilon} \{j\omega g_{11}(o,j\omega)\} \to -\{1 + \varepsilon\exp(-L)\exp(-j\omega L)\} \qquad (63)$$

An identical expression may also be derived for the H.F. limit of $g_{22}(o,j\omega)$. Diverging loops* on the inverse Nyquist loci of $g_{11}^{-1}(o,j\omega)$ and $g_{22}^{-1}(o,j\omega)$ may therefore be anticipated to become increasingly noticeable as L is reduced, each loop occupying a frequency increment $\Delta\omega \simeq 2\pi L^{-1}$.

9.3 Inverse Nyquist Loci

Two examples of the loci of $g_{11}^{-1}(o,j\omega)$ and $g_{22}^{-1}(o,j\omega)$ computed from (53) and (54) are given in Figs. 3,4,5 and 6, the so called 'short' column parameters being $\varepsilon = 0.75$, $L = 2.8$ whilst for the 'longer' column, $\varepsilon = 1.0$ and $L = 5.0$. $T = 5.0$ in both cases. The stronger wave effects on g_{11}^{-1} in the short column case are obviously present, whilst in the longer column (which has a positive $g_{11}(o,o)$) nonminimum-phase behaviour of g_{11} is clearly predicted by virtue of

* Simplified H.F. analysis (similar to that carried out in the companion paper) may be carried out by ignoring all dependent variables in p.d.e. (30) (Laplace transformed in p. w.r.t. τ) not multiplied by p, giving, with $c = 1.0$,:

$$\lim_{|p|\to\infty}(p\, g_{11}) = \lim_{|p|\to\infty}(p\, g_{22}) = -1.0$$

Such analysis clearly predicts the negative integrating behaviour of the process at H.F. but fails to reveal the travelling wave effects.

the locus orbiting the origin. The loci predictions are borne out by the unit-step-responses computed directly from the p.d.e's (30) for identical parameters and shown in Figs. 7 and 8. The nonminimum phase behaviour of g_{11} for the large column is obvious. The steady-states and basic time-constants of the step-responses are likewise found to be in accordance with locus predictions.

The inverse Nyquist loci are thus confirmed by the analysis of Section 9.2 and by step response tests. Being of an open-loop nature however, the latter do not bring out the wave motions within the column, predicted by analysis. These acquire significance once closed-loop control is applied and it is readily shown from (63) that, in the shorter column, taking feedback temperature measurements at, say, h = 0.5L (= 1.0) would generate an additional H.F. phase-lag ϕ, $\left[= \sin^{-1} \{\varepsilon \exp(-L+h)\}\right]$, of 22^{o} in this case.

Twin product control of packed columns is therefore made difficult by additional phase-lag due to travelling waves in shorter towers and by the non-minimum-phase behaviour of g_{11} in taller plants. Neither problem was revealed by similar analysis of tray columns in the companion paper. In practice, however, the continuous equilibrium assumption made for the tray column may not be realised leading to behaviour somewhere between the two idealised cases studied here.

9.4 Non-minimum-phase behaviour of g_{11}: A physical explanation

The initial negative response of $y(o,\tau) - x'(o,\tau)$ (i.e. the negative H.F. gain of $g_{11}(o,j\omega)$) is readily explained in physical terms. When V_s and L_r are simultaneously increased, (i.e. $v+\ell > 1.0$), weak vapour from the bottom of the column will be moved initially upwards, whilst rich liquid will be moved initially downwards so reducing $Y(o) - X'(o)$. Only then, will the cross-flow between liquid and vapour commence to change towards the new operating condition, the final extent of this change depending on column parameters. Accepting

that the final response may be positive, with a sufficient value of L, then the predicted non-minimum-phase response is explained. The argument does not rely on the assumption that c = 1.0, or indeed that c = any specific value.

9.5 Low-frequency (L.F.) behaviour: Effect of Terminal Capacitance

Additional features of the system frequency response can be deduced directly from expressions (53) and (54) without needing computation: we have so far deduced only the zero frequency and H.F. response. In particular the L.F. behaviour of the system may be examined by retaining the first power of p in approximating these expressions as $p \to 0$. Such a procedure applied to (53) leads to the result

$$g_{11}^{-1}(o,p) \to g_{11}^{-1}(o,o)(1+T_2p)/(1+T_1p) \quad , \quad L|p| << 1.0 \tag{64}$$

where

$$\left.\begin{aligned} T_1 &= -L^2\{2L(\alpha+1) - 3\varepsilon\}/6\{\varepsilon L^2 - (\alpha+1)L - \varepsilon/2\} \\ T_2 &= L\{(\alpha+1)L + \varepsilon\}/(2\varepsilon L + \alpha + 1) \end{aligned}\right\} \quad (T = 0) \tag{65}$$

or

$$T_1 = T \ , \quad T_2 = \alpha T(2L+1)/(2\varepsilon L + \alpha + 1) \quad , \quad T >> 1 \tag{66}$$

so that, for small $|p|$

$$g_{11}^{-1}(o,p) \simeq g_{11}^{-1}(o,o)\{1 + (T_2 - T_1)p\} \tag{67}$$

As with tray-columns therefore, end-vessel capacitance, affects only the L.F. response and hence the final tail of the step-response, this prediction being confirmed by the step-responses of Fig. 9, for L = 5, ε = 1.0.

In addition we note that, provided

$$T_2 > T_1 \tag{68}$$

then the direction of locus departure from the point $g_{11}^{-1}(o,o) + jo$ is $+90^o$ for $g_{11}(o,o) > 0,0$ (i.e. for long columns) and -90^o for $g_{11}(o,o) < 0.0$ (i.e. for short columns), in accordance with the computed loci of Figs. 4 and 3 respectively: and again confirming the non-minimum-phase nature of g_{11} for long columns. Constraint (68) is clearly satisfied in the presence of T, provided L > 0.5, and for very large and very small L when T = o. Intermediate

cases need deeper investigation.

10. Unequal Vapour and Liquid Capacitance ($c \neq 1.0$)

Predictions made so far have been for the special case $c = 1$. This case was chosen to ease mathematical derivation. The conditions can be approached practically (see for instance Strigle and Perry (4)) but is atypical of common practice where c is generally far smaller than unity. Fortunately, the system behaviour is not greatly sensitive to wide variations in c, as will be demonstrated.

Once we set $c \neq 1.0$, calculations on the lines set out in Section 8 can still be carried out but, because of the loss of absolute symmetry, the system matrices are no longer readily diagonalised and analytic expressions become much more cumbersome. Care and algebraic persistance are all that is required however, to yield ultimately[3] the solution for $\underline{G}(o,p)$ given in matrix equation (69). It is readily checked that the off-diagonal terms become zero at $p = o$ and $g_{11}(o,p)$ and $g_{22}(o,p)$ are identical to the values given for the $c = 1$ case (equations 55 and 56) as would be expected since capacitance should not influence the steady-state gains. At higher-frequencies, however, the T.F.M. ceases to be diagonal since the plant is now symmetrical only for $p = o$, whereas with $c = 1$ symmetry clearly pertains for all frequencies.

If, as an extreme example, we consider $c = o$, then from (69) we can deduce[2] that

$$\lim_{\omega \to \infty} \underline{G}(o,j\omega) = \frac{\alpha \exp(-2L) - 1 - 1.5\varepsilon\exp(-L)}{2} \begin{pmatrix} 1 & 1 \\ 1 & 1 \end{pmatrix} + \frac{\varepsilon\exp(-L)\exp(-j\omega L)}{4} \begin{pmatrix} -1 & 1 \\ 1 & -1 \end{pmatrix} \tag{72}$$

so that the four Nyquist loci converge to small orbits of radius $\varepsilon\exp(-L)/4$ about the real point $-\{1 + 1.5\ \varepsilon\ \exp(-L) - \alpha\ \exp(-2L)\}/2$. The result is simply checked from the original p.d.e's (30) noting that, immediately following step-changes v and ℓ, the liquid composition changes, and hence y_e and x' will remain zero initially because of liquid capacitance. Furthermore

$$\underline{G}(o,p) = \frac{1}{1+c+cp}\begin{pmatrix}\cosh PL & \sinh PL\\ \sinh PL & \cosh PL\end{pmatrix}.$$

$$\begin{pmatrix}
\dfrac{(1+c)\cosh qL\left[(\varepsilon+\frac{\alpha-c}{2}p)e^{PL}+(\varepsilon-\frac{1-c\alpha}{2}p)e^{-PL}\right]-q\sinh qL\left[(\alpha+c)e^{PL}+(1+c\alpha)e^{-PL}\right]-\varepsilon(1+c)\left[2+(1+c+\frac{cp}{2})p\right]}{(1+c)p(1+\alpha^{-1}h_e)\cosh qL+2q(1-\alpha^{-1}h_e)\sinh qL} \\
\dfrac{(1+c)\cosh qL\left[(1+\alpha+\frac{\alpha+c}{2}p)e^{PL}-(1+\alpha+\frac{1+c\alpha}{2}p)e^{-PL}\right]-q\sinh qL\left[(\alpha-c)e^{PL}+(1-c\alpha)e^{-PL}\right]-\varepsilon(1-c^2)p/2}{(1+c)p(1+\alpha^{-1}h_e)\cosh qL+2q(1-\alpha^{-1}h_e)\sinh qL} \\
\dfrac{q\cosh qL\left[(\alpha+c)e^{PL}-(1+c\alpha)e^{-PL}\right]-(1+c)\sinh qL\left[(\varepsilon+\frac{\alpha-c}{2}p)e^{PL}+(-\varepsilon+\frac{1-c\alpha}{2}p)e^{-PL}\right]-\varepsilon(1-c)q}{(1+c)p(1+\alpha^{-1}h_e)\sinh qL+2q(1-\alpha^{-1}h_e)\cosh qL} \\
\dfrac{q\cosh qL\left[(\alpha-c)e^{PL}-(1-c\alpha)e^{-PL}\right]-(1+c)\sinh qL\left[(1+\alpha+\frac{\alpha+c}{2}p)e^{PL}+(1+\alpha+\frac{1+c\alpha}{2}p)e^{-PL}\right]-2\varepsilon q(1+c+\frac{cp}{2})}{(1+c)p(1+\alpha^{-1}h_e)\sinh qL+2q(1-\alpha^{-1}h_e)\cosh qL}
\end{pmatrix} \tag{69}$$

where $P = \frac{1-c}{2}p$ (70) and $q = \sqrt{(1+c)p(4+p+cp)/4}$ (71)

terminal capacitance will keep $y_e(o)$ and $x'_e(o)$ at zero initially. Transformed p.d.e's (31) and (32) thus yield the following vapour-change equations:

$$(1 - s)\tilde{\tilde{y}} = - \tilde{y}(o) - \tilde{z}_1/s \tag{73}$$

and

$$(1 + s)\tilde{\tilde{x}}'_e = - \tilde{z}_1/s \tag{74}$$

which may be solved subject to the feed boundary equations (30) and (40) to give

$$\tilde{y}(o) = - \{1.5\,\varepsilon\exp(-L) + 1 - \alpha\exp(-2L)\}\tilde{z}_1 \tag{75}$$

or, knowing that $\tilde{x}'(o) = o$ initially,

$$\begin{pmatrix} \tilde{y}(o) - \tilde{x}'(o) \\ \tilde{y}(o) + \tilde{x}'(o) \end{pmatrix} = \frac{-\{1.5\varepsilon\exp(-L) + 1 - \alpha\exp(-2L)\}}{2} \begin{pmatrix} 1 & , & 1 \\ 1 & , & 1 \end{pmatrix} \begin{pmatrix} \tilde{z}_1 + \tilde{z}_2 \\ \tilde{z}_1 - \tilde{z}_2 \end{pmatrix} \tag{76}$$

Apart from the small orbital terms therefore, the initial unit step-response of the system obtained from (76) is identical to Lim $\underline{G}(o,j\omega)$ as $\omega \to \infty$.

This predicted initial value compares most favourably with the initial negative step-response obtained by numerical simulation typified by Fig. 10 which also shows the computed response of g_{11} for various values of $0 < c < 1.0$. for the case of $L = 5$, $\varepsilon = 1.0$, $T = 5$. It is interesting to note the persistence of the initial negative dip in the responses despite the variation in **c**: This is not therefore a feature of the c = 1 case alone.

Fig. 11 compares the loci of $g_{11}^{-1}(o,j\omega)$ for the two extreme cases of c = 0.0 and c = 1.0 computed from equations (69) and (53) respectively for the same parameters as used for Fig. 10. The similarity of the loci confirms the similar transient responses, the finite negative destination of the c = o locus merely indicating the abrupt negative initial step-response rather than the slightly more gradual initial response exhibited when c > o.

It should, of course, be noted that in the situation c = 0.0, since T.F.M. $\underline{G}(o,j\omega)$ is nondiagonal, $g_{11}^{-1}(o,j\omega)$ is the inverse Nyquist locus between $y(o) - x'(o)$ and $v + \ell$ only when input $v - \ell = o$, i.e. when $y(o) + x'(o)$ is totally uncontrolled. It is therefore important also to examine the locus produced when output $y(o) + x'(o)$ is under control and, as an extreme case,

we consider $y(o) - x'(o) = 0$, {i.e. $y(o)$ $x'(o)$ perfectly controlled}. Under these circumstances it is readily shown that the inverse transfer-function between $y(o) - x'(o)$ and $v + \ell$ becomes $g^{*}_{11}(o,j\omega)$ where

$$\underline{G}^{-1}(o,j\omega) = \underline{G}^{*}(o,j\omega) = \begin{bmatrix} g^{*}_{11}(o,j\omega) & , & g^{*}_{12}(o,j\omega) \\ g^{*}_{21}(o,j\omega) & , & g^{*}_{22}(o,j\omega) \end{bmatrix}$$

$$= \frac{1}{\{g_{11}(o,j\omega)g_{22}(o,j\omega) - g_{12}(o,j\omega)g_{21}(o,j\omega)\}} \begin{bmatrix} g_{22}(o,j\omega) & , & -g_{12}(o,j\omega) \\ -g_{21}(o,j\omega) & , & g_{11}(o,j\omega) \end{bmatrix} \qquad (77)$$

The locus of $g^{*}_{11}(o,j\omega)$ derived from (69) and (77) is compared with that of $g^{-1}_{11}(o,j\omega)$ in Fig. 12 for $c = o$, $L = 5$, $\varepsilon = 1$ and $T = 5$. The obvious similarity of shape and frequency calibration over a wide range further justifies the prediction (from Fig. 11) of similarity of transient behaviour for any c in the range $o < c < 1.0$ (observed in Fig. 10).

11. Reconciling the Predicted Behaviour of Tray and Packed Columns

In Section 10 we have shown that the predicted behaviour of packed columns is not highly sensitive to variations in c. The qualitative explanation of Section 9.4 was likewise independent of c. The assumption that $c = o$ made in tray column analysis is therefore not the source of behavioural difference between the two types of column. An examination of both the derived inverse Nyquist loci and simulated time responses of the two types indicates that it is the parameter L which chiefly controls the response differences. Furthermore as L is increased the behaviour of packed and tray columns approach equality. This is here demonstrated by Fig. 13 which shows how, as L increases from 5 to 7 for a packed column ($c = 1$, $\varepsilon = 1.0$), there is a movement of the locus of $g^{-1}_{11}(o,j\omega)$ away from the origin and towards the much straighter tray column locus ($L = 10$, $\varepsilon = 0.1$) of similar gain. This suggests a reduction in the nonminimum phase dip of the transient response of $y(o) - x'(o)$ as L increases

and this is dramatically confirmed by the computed step responses of Fig. 14 for L = 20, for packed and tray columns of identical static gain. The effect of c = change is also shown. That L should be the controlling parameter (for packed and tray column discrepancies) is not surprising with hindsight: Recalling that L = L'k/V for the packed column then, for a given real length L' and vapour rate V, an increase of L implies an increase in evaporation coefficient k and hence column operation closer to equilibrium at all points in the tower. An increase in L for packed columns thus causes a closer approach to the operating condition (i.e. continuous equilibrium) assumed in tray column analysis.

12. Conclusions

A parametric 2x2 T.F.M. model for packed distillation columns, (derived completely analytically and precisely), has been presented for columns that are built and operated symmetrically. Apart from the symmetry assumption, all other assumptions, made entirely and only at the outset, are those which have been adopted in part analytic studies of previous investigators. The model should apply as a good approximation to towers operated with a reasonable degree of assymmetry.

The calculation of the T.F.M. was illustrated for the special case of dynamic symmetry, i.e. for a vapour/liquid capacitance ratio, c, = 1.0 in the interests of simplicity of analysis. The result for general c is stated and interested readers may acquire its derivation via references (2) and (3).

If the chosen outputs and inputs are $[y(o) - x'(o), y(o) + x'(o)]^T$ and $[v + \ell, v - \ell]^T$ then the T.F.M. is found to be diagonal, (as for the tray columns case[1]) over the entire frequency range, if c = 1. When $c \neq 1$, the T.F.M. is diagonal only at zero frequency, but comparison of the inverse Nyquist loci of the c = 1 and c = o cases indicates that variation of c does not greatly affect system behaviour.

An essential difference revealed between packed and tray columns is the appearance of a nonminimum phase response of $y(o) - x'(o)$ to $v + \ell$ in the $c = 1.0$ case. The associated negative dip in the step-response is found to persist (and increase slightly) when c is reduced in the range $0.0 \leq c \leq 1.0$. This characteristic suggests potential difficulties in controlling product separation in packed columns. Indeed the static 'tilt' or separation gain can vary in sign depending on parameter values and, for short columns, becomes negative, thus eliminating the nonminimum-phase behaviour under these circumstances. Short columns however, have been shown to produce other problems, i.e. travelling wave phenomena which can contribute additional phase-shift of some 22^{o} and which should be accounted for in controller design.

The possibility of zero separation-gain clearly arises, depending on plant and mixture parameters and upon operating conditions. This could explain the practical difficulties in controlling this quantity sometimes experienced in practice: even in tray columns which never operate in precise equilibrium.

Because of wave effects in short packed columns and nonminimum phase behaviour in larger towers, approximate (e.g. first-order lag) models should be applied with caution to the twin product control problem. Such models will apply only for restricted ranges of controller gain.

It has been shown that normalised length parameter L ($=L'k/V$) is that which controls the discrepancy between packed and tray columns model predictions. As might be expected, increase of L (i.e. by increase of evaporation constant k in a given column) brings the frequency and transient responses of the two types of column into close proximity. It does not, however, completely eliminate the nonminimum phase response of $y(o) - x'(o)$ which arises basically from the essential nonequilibrium of packed column operation.

Finally we should stress that the control problems raised by this analysis apply to two-product control and not necessarily to single-product control.

13. References

(1) Edwards, J.B. and Tabrizi, M.H.N., 'The calculation and interpretation of parametric transfer functions for binary distillation columns of the tray type ', Trans. Inst. Chem. Engrs.

(2) Edwards, J.. and Guilandoust, M., 'The influence of vapour capacitance on the composition dynamics of packed distillation columns', University of Sheffield, Dept. of Control Eng.,Research Report No. 166, Nov. 1981, 15 pp.

(3) Guilandoust, M., Edwards, J.B., 'A parametric transfer-function matrix for packed binary distillation columns having unequal vapour and liquid capacitance', ibid, Research Report No. 171, February 1982.

(4) Strigle, R.F. and Perry, D.A., 'Packed towers reduce cost', Hydrocarbon Processing, Vol. 60, No. 2, p. 101, 1981.

Fig. 1 Illustrating the complete system

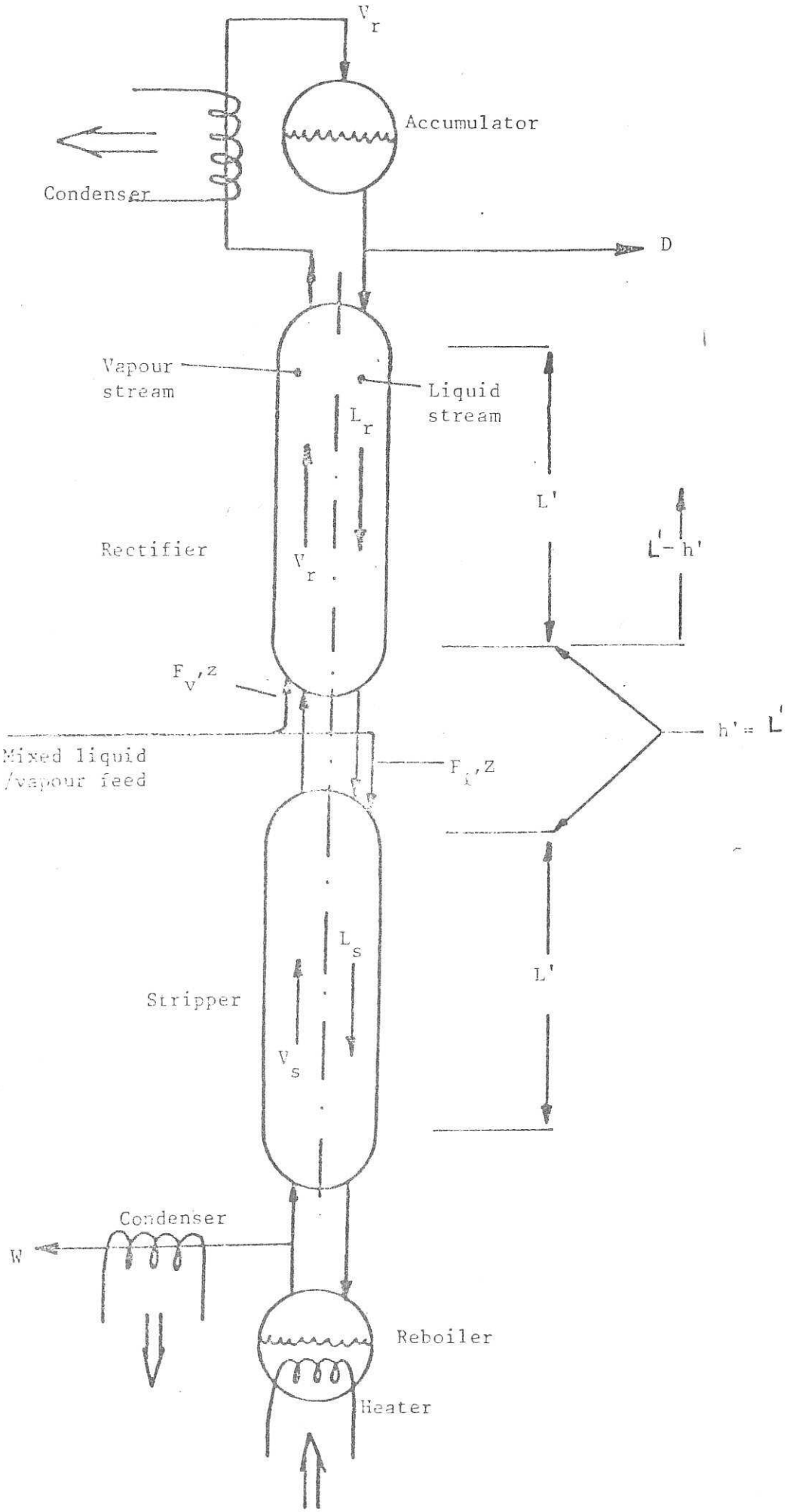

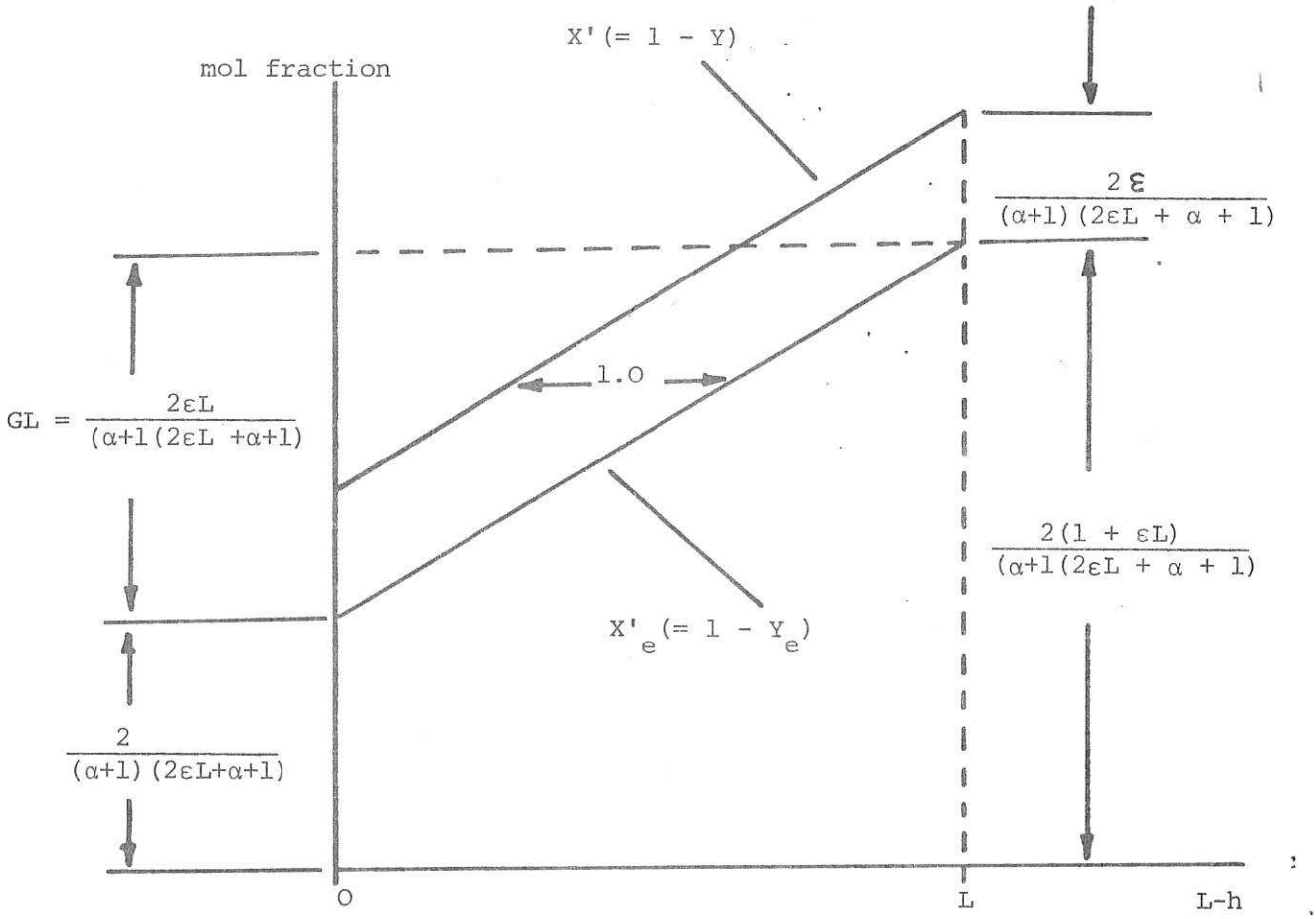

Fig. 2 Steady-state composition profiles

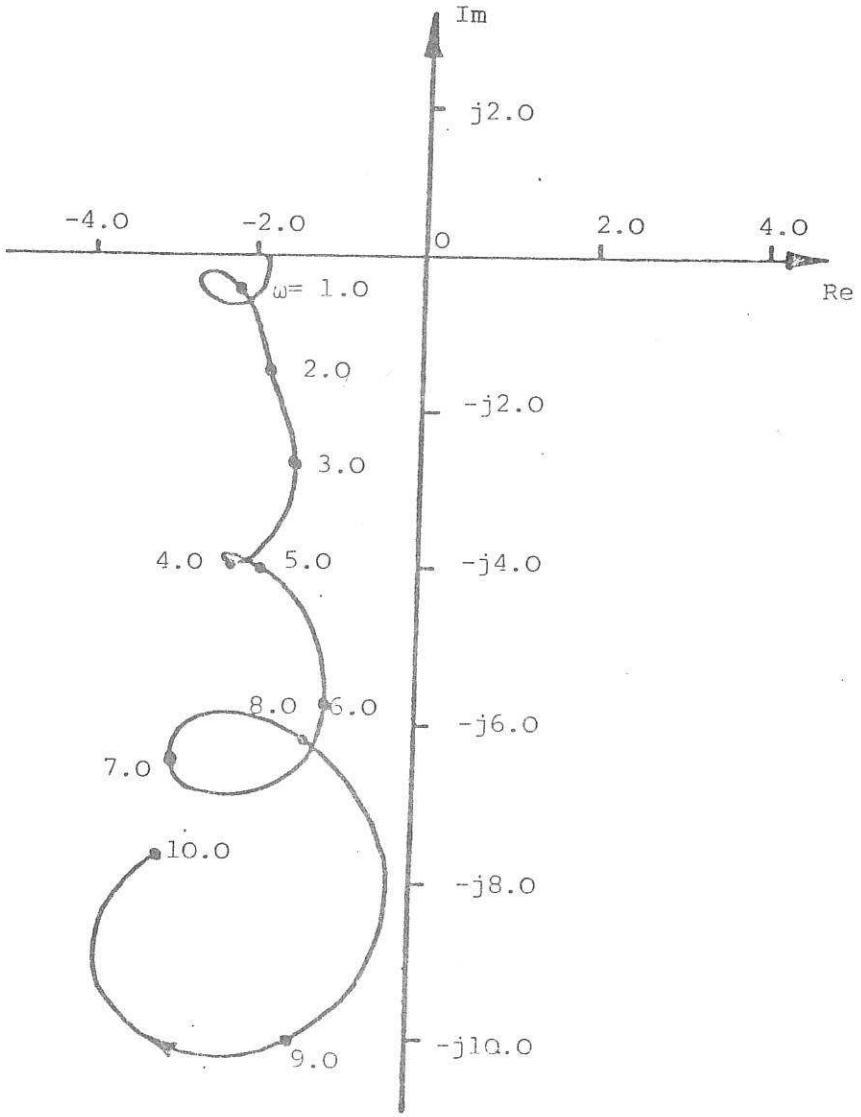

Fig. 3. Inverse Nyquist locus of $g_1^*(o,j\omega)$ for shorter column

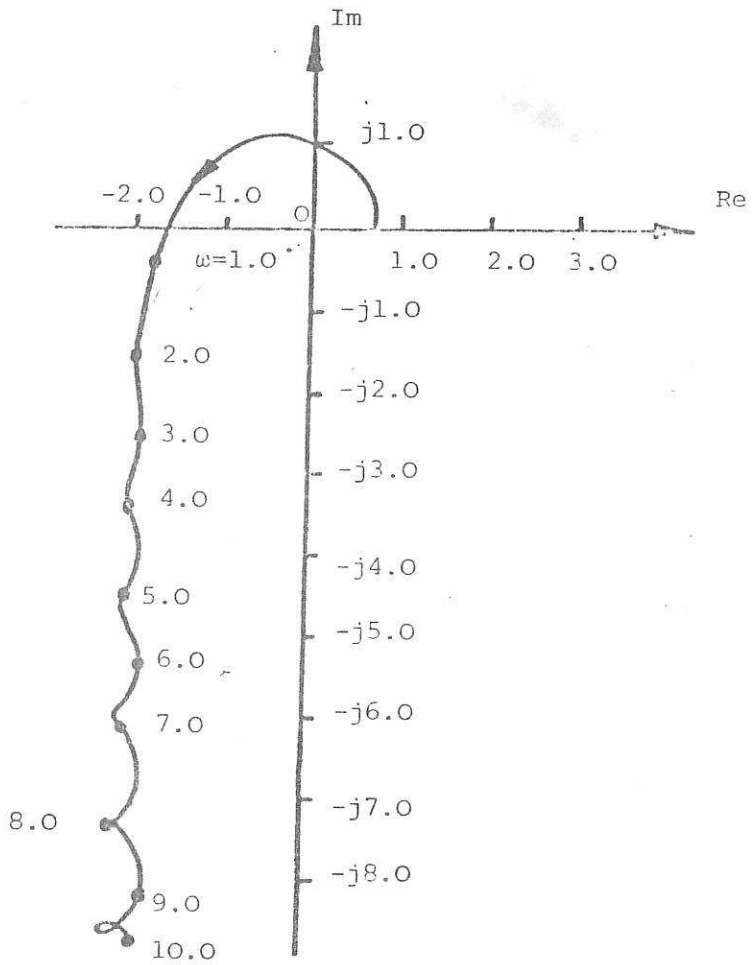

Fig. 4. Inverse Nyquist locus of $g_1^*(o,j\omega)$ for longer column

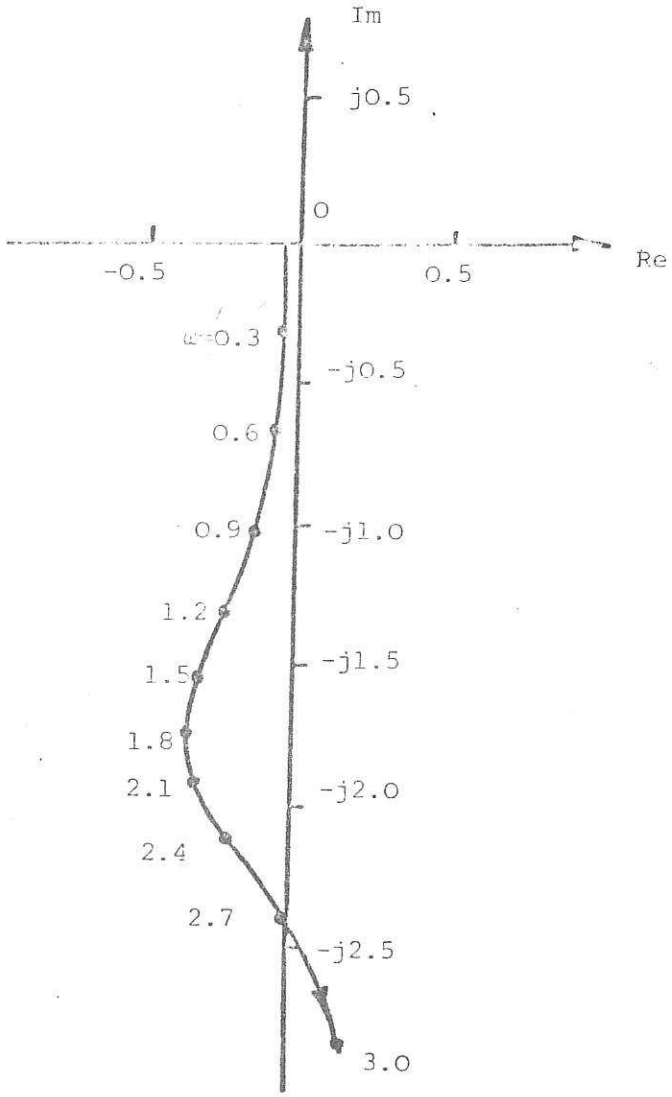

Fig. 5 Inverse Nyquist locus of $g_2^*(o,j\omega)$ for shorter column

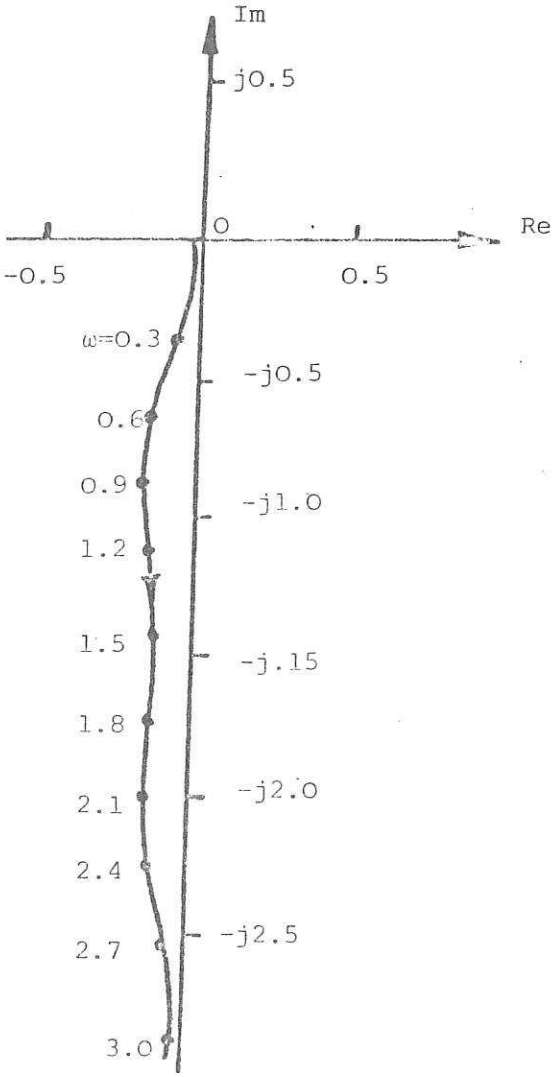

Fig. 6 Inverse Nyquist locus of $g_2^*(o,j\omega)$ for longer column

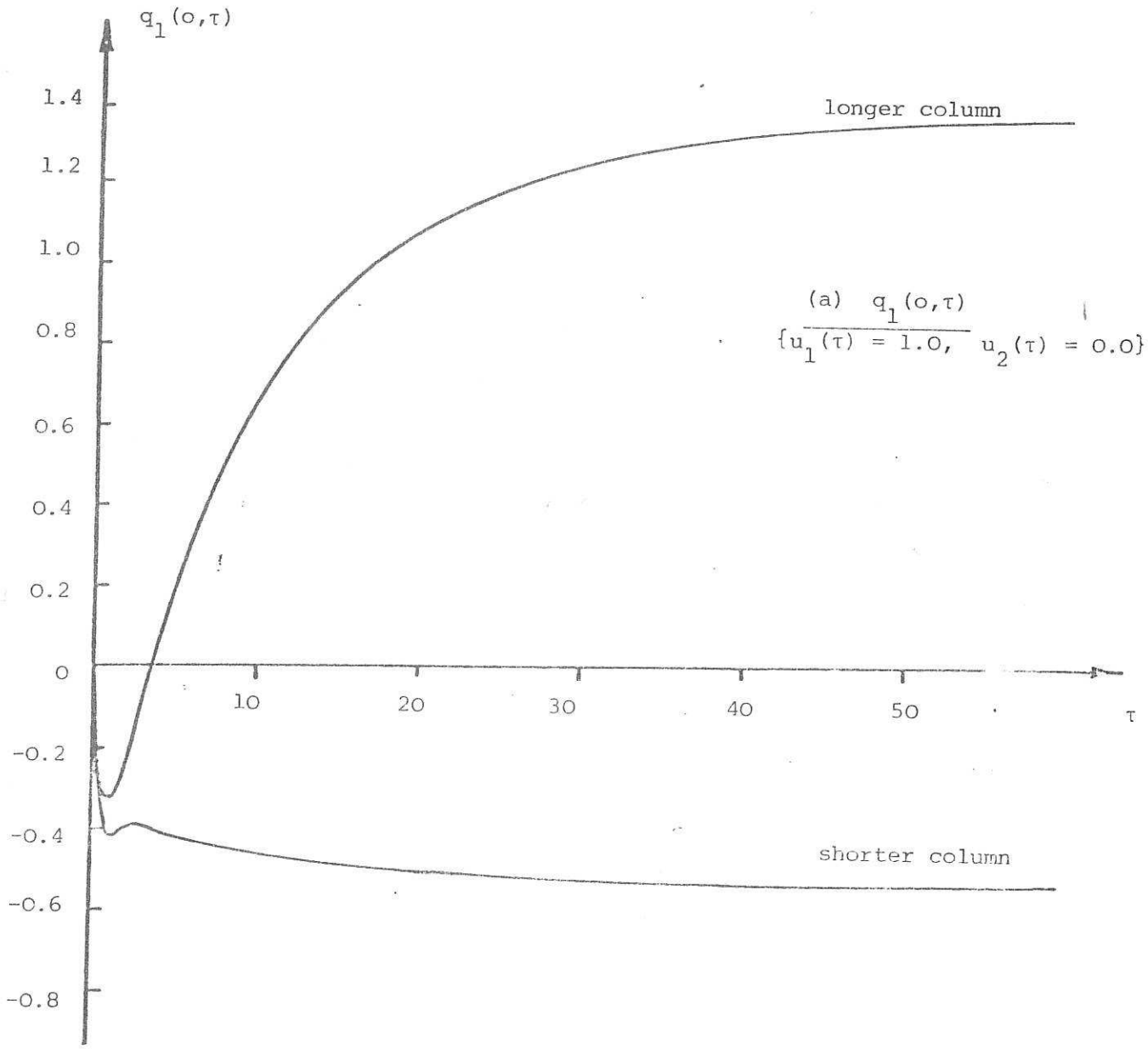

Fig. 7. Unit-step responses

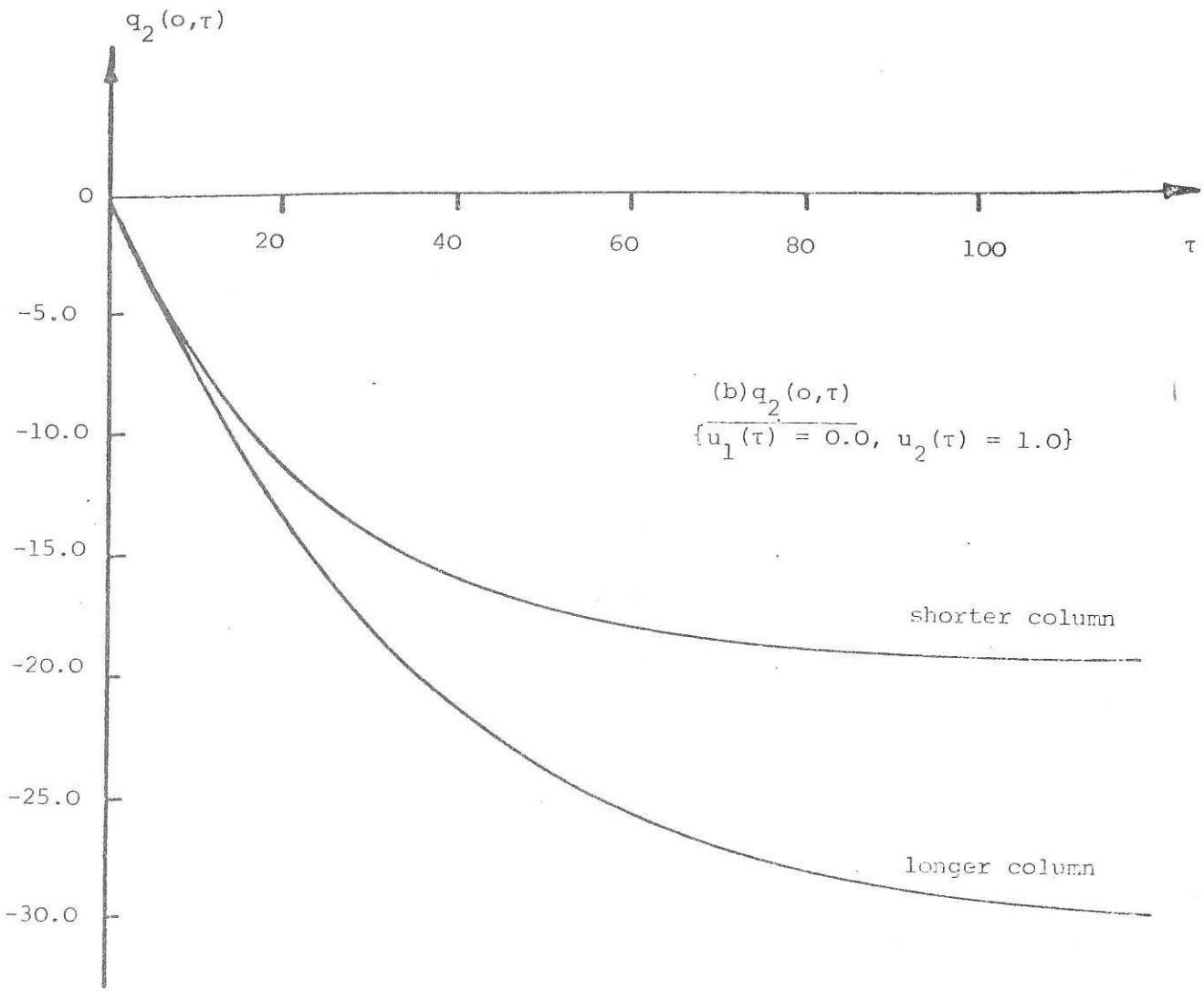

Fig. 8. Unit-step responses

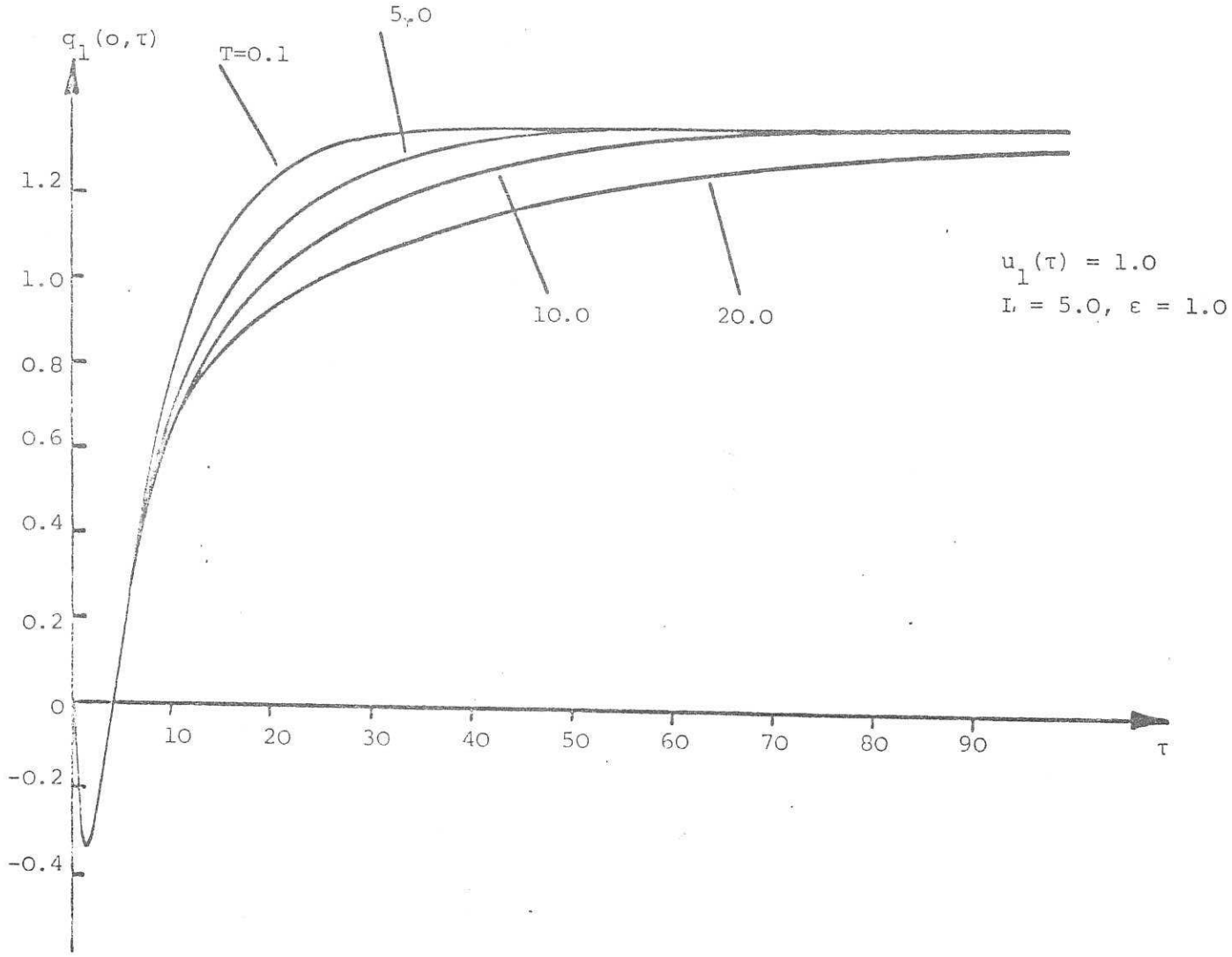

Fig. 9 Unit step responses for various end-vessel capacitances

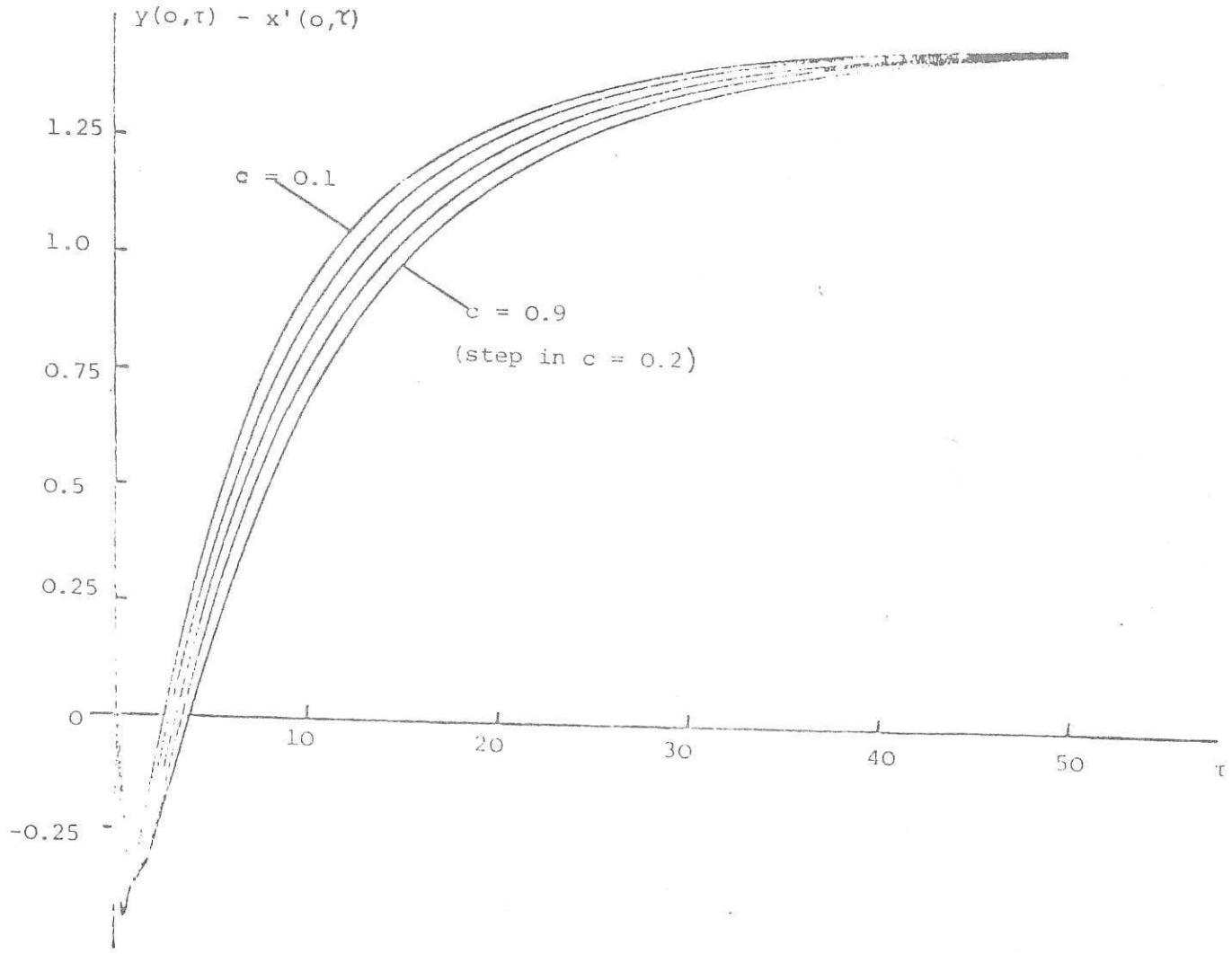

Fig. 10. Effect of varying capacitance ratio c on response of $y(o,\tau) - x'(o,\tau)$ to unit step in $z_1 + z_2$

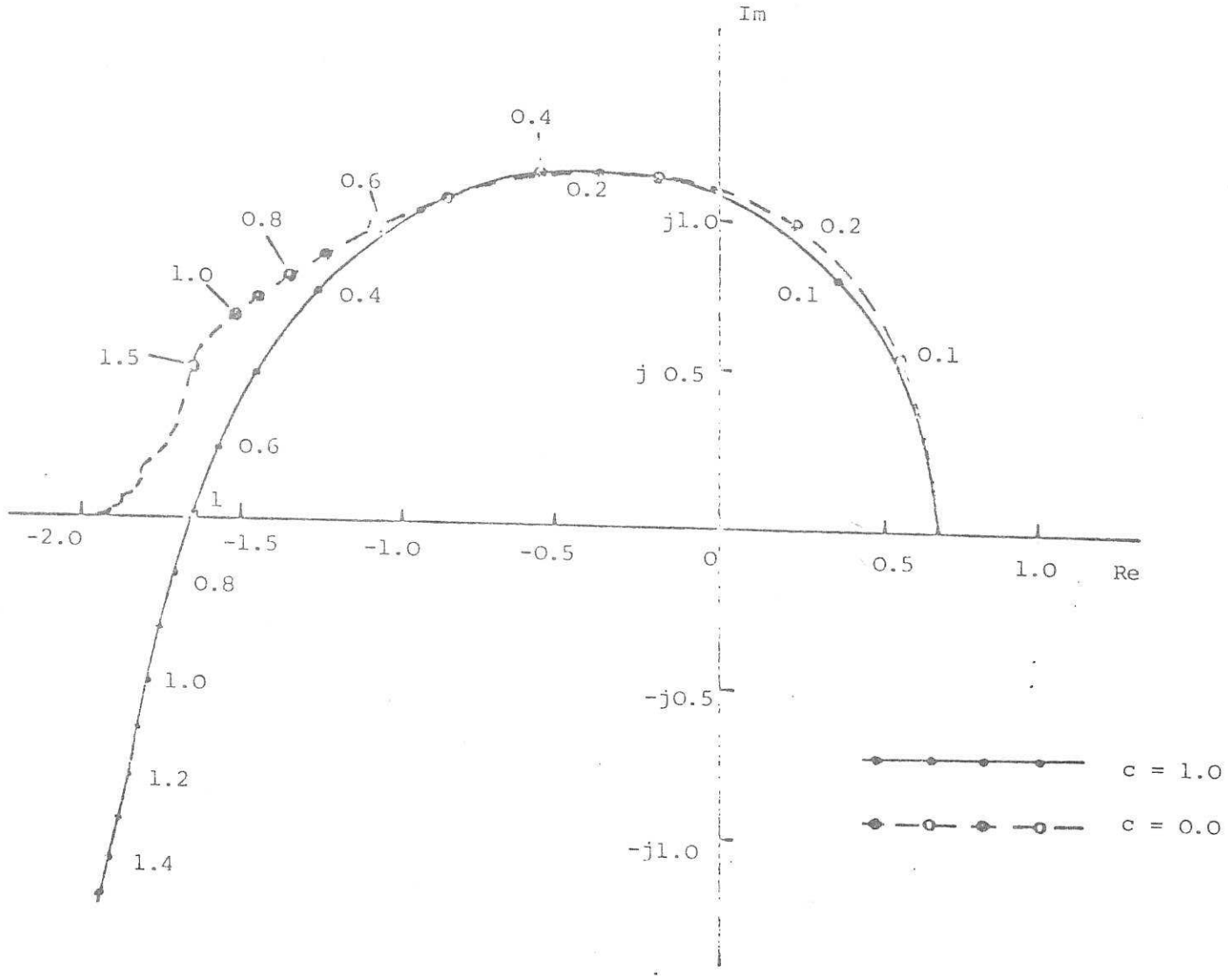

Fig. 11. Loci of $g_{11}^{-1}(o,j\omega)$ for c = 0.0 and c = 1.0

Fig. 12. Comparing loci of $g_{11}^{-1}(o,jw)$ and $g_{11}^{*}(o,jw)$ for c = 0.

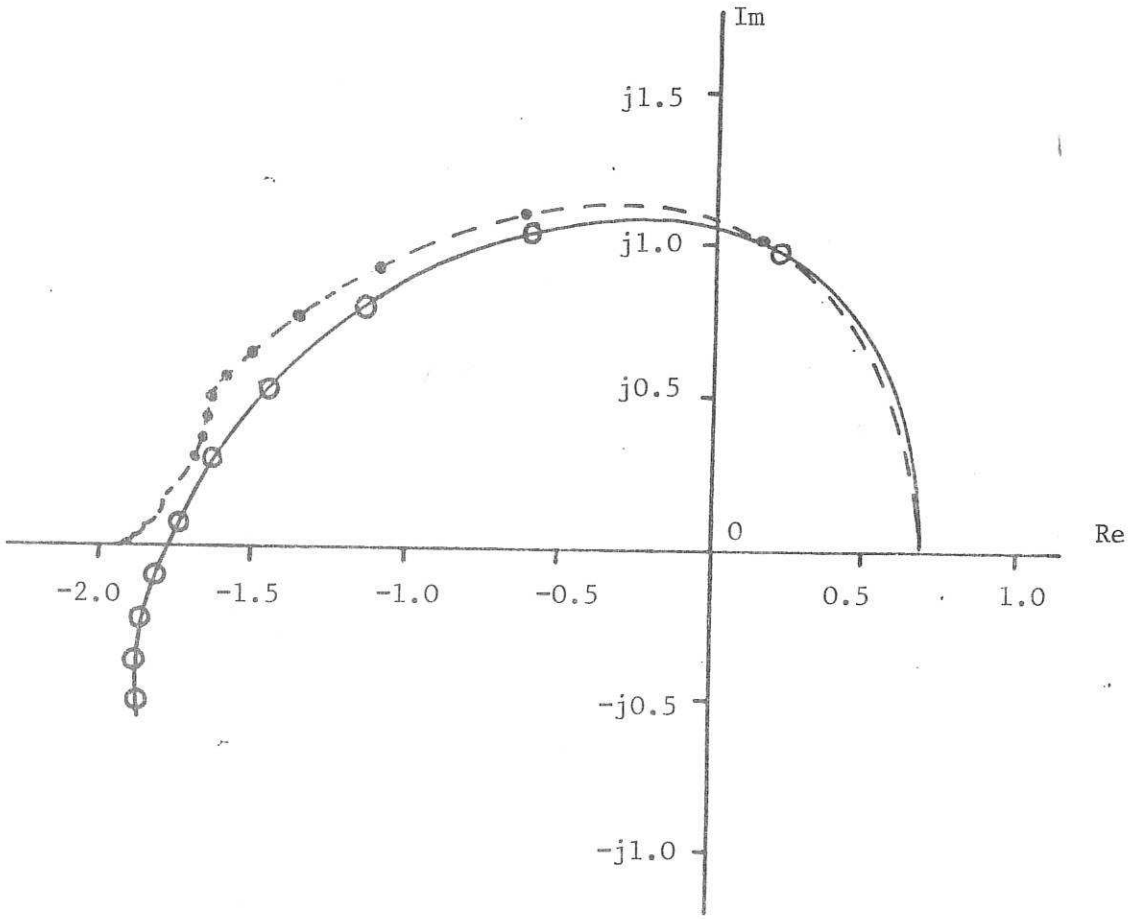

Key:

$g_{11}^{-1}(o,jw)$ - $0 \leq w \leq 2$, $\Delta w = 0.2$

$g_{11}^{*}(o,jw)$

L = 5, T = 5, ε = 1.0